CHIN. PHYS. LETT. Vol. 37, No. 7 (2020) 073201

Deceleration of Metastable Li^+ Beam by Combining Electrostatic Lens and Ion Trap Technique

Shao-Long Chen(陈邵龙)[1], Peng-Peng Zhou(周朋朋)[1,2], Shi-Yong Liang(梁世勇)[1,2], Wei Sun(孙伟)[1], Huan-Yao Sun(孙焕尧)[1], Yao Huang(黄垚)[1], Hua Guan(管桦)[1*], Ke-Lin Gao(高克林)[1,3*]

[1]*State Key Laboratory of Magnetic Resonance and Atomic and Molecular Physics, Wuhan Institute of Physics and Mathematics, Innovation Academy for Precision Measurement Science and Technology, Chinese Academy of Sciences, Wuhan 430071, China*

[2]*University of Chinese Academy of Sciences, Beijing 100049, China*

[3]*Center for Cold Atom Physics, Chinese Academy of Sciences, Wuhan 430071, China*

(Received 31 March 2020; accepted 8 May 2020; published online 21 June 2020)

Ion deceleration has played a critical role in ion-related research when the ions are produced in the form of a high-energy beam. We present a deceleration method combining electrostatic lens and ion trap technique, which can effectively decelerate ions to energy below the trapping potential of a typical ion trap. The experiments were performed on metastable $1s2s\,^3S_1$ Li^+ ions, and demonstrated that the kinetic energy could easily be reduced from ∼450 eV to a few eV, with the latter being confirmed using the Doppler-shifted fluorescence spectra.

PACS: 32.70.−n, 32.70.Jz, 32.10.Fn, 07.75.+h DOI: 10.1088/0256-307X/37/7/073201

There has been enormous progress in ion trap technology, which has demonstrated an unprecedented level of control over the system under study. It been applied to perform ultra-high precision spectroscopic measurements of ions trapped and cooled in an ion trap. While many such experiments have been performed with substantial success in recent years, problems have arisen when the ions under investigation could not be produced directly in the trap.[1−6] For example, in recent decades, highly charged ions (HCIs) have gained increased attention from scientists for their potential for realizing frequency uncertainties at a level below a few parts in 10^{-19} and a high sensitivity to effects beyond the standard model.[7,8] Moreover, HCIs generated from an electron beam ion trap or electron cyclotron resonance should be decelerated before they can be trapped and cooled.[6] Another example is Li^+, which is one of the simplest atomic systems. Its attractive measurements of $1s2s\,^3S_1 \rightarrow 1s2p\,^3P_{0,1,2}$ transitions have gained interest for decades because of their significance in the rigorous testing of relativistic quantum theory, including quantum electrodynamics, as well as their correlations within a multi-electron system. To date, most measurements of these transitions have been performed on ion beams generated from atomic beams,[9−12] which limited the accuracy due to various spectral line broadening and shifts. Recently, it has been proposed that by trapping and sympathetic cooling metastable Li^+ ions in a linear Paul trap, ultra-high precision spectroscopic measurements are possible, and the trapped and sympathetically cooled Li^+ have been reported.[13] Generally, the metastable Li^+ ion is generated using electron bombardment and extracted with high kinetic energy, since the energy level of the metastable Li^+ ion is 59 eV above the ground level.[14] Thus, a deceleration system is required to slow down the ions for further sympathetic cooling and precision spectroscopy measurement.

Ion deceleration has been widely studied in highly charged ions,[1,3,6] the interaction of ions and matter,[15,3] atomic precision spectroscopy,[16,7] and state-selective charge transfer.[5] The most commonly used methods for this are electron cooling,[17] and electrostatic lens and laser cooling.[18] The former method is used for ion deceleration in storage rings, and the latter is usually used for trapped ions. Here, for ion beams, the common deceleration method is use of the electrostatic lens. Previous experiments have used different electrostatic lenses, and ion energy of 1 eV to tens of eV has been reported.[1−3,15,19−23] However, an electrostatic lens cannot filter noises, particularly neutral particle noises which affect the experiments to a greater or lesser degree. These noises exist in the electron ionization and chemical ionization ion source because of the reagent and background gases, and transit in a straight line out-controlled by the electro–magnetic field.[24,25] Here, a curved quadrupole[26−32] offers a good solution for filtering the neutral noise. Moreover, as a two-dimensional ion trap, the curved quadrupole can filter the high energy ions when the radio frequency (RF) and direct current (DC) fields

Supported by the Scientific Instrument Developing Project of the National Natural Science Foundation of China (Grant Nos. 11934014, 11622434, and 11804373), the Scientific Instrument Developing Project of the Chinese Academy of Sciences (Grant No. YZ201552), the Strategic Priority Research Program of the Chinese Academy of Sciences (Grant Nos. XDB21010400 and XDB21030300), CAS Youth Innovation Promotion Association (Grant Nos. Y201963 and 2018364), and the Hubei Province Science Fund for Distinguished Young Scholars (Grant No. 2017CFA040)

*Corresponding authors. Email: guanhua@wipm.ac.cn; klgao@wipm.ac.cn

© 2020 Chinese Physical Society and IOP Publishing Ltd

are set at an appropriate level.

In this study, we describe a method that combines the electrostatic lens and ion trap techniques. The former is used to focus the beam and to decelerate the ions, whereas the latter filters out the neutral particles and high-energy ions with specific potential well depth. By using this method, we decelerated the metastable Li^+ ions generated by an electron impact,[16] and the kinetic energy of the ions was slowed to a few eV, which is crucial for the subsequent Li^+ ion sympathetic cooling and precision spectroscopy measurements. Additionally, this method is feasible for other experiments wherein ions need to be decelerated to a low kinetic energy.

A schematic of the deceleration setup is shown in Fig. 1, which comprises a drift tube, an electrostatic lens, and a curved quadrupole. The drift tube has a length of 100 mm, with inner and outer diameters of 15 mm and 21 mm, respectively. A suitable voltage is applied to the tube through a high-voltage power supply (ISEG NHS 6000 N) to guide the ions through a certain space and into the electrostatic lens.

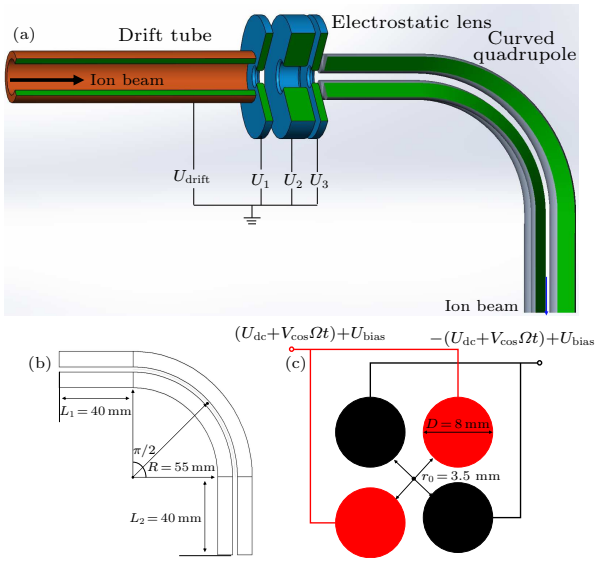

Fig. 1. (a) Sectional view of the deceleration device; (b) top view of the curved quadrupole; (c) cross section of the curved quadrupole and the connection of the DC and RF potentials.

The electrostatic lens comprises three round plates with holes in the center, and the three concentric plates with the drift tube are powered by the same source as the drift tube, but through different channels. The ions can be decelerated and injected into the curved quadrupole at a minimum loss by adjusting the voltage applied on each plate.

The curved quadrupole comprises four curved rods, and its structure and dimensions are shown in Figs. 1(b) and 1(c). Moreover, Fig. 1(c) also shows the RF and DC voltage as well as a DC bias voltage (U_{bias}) applied on the electrodes. The DC voltages and RF are adjusted to allow the desired ions to pass through the quadrupole with the best transmission efficiency.

To detect the beam intensity of the decelerated ions, a Faraday cup is placed ~10 mm away from the exit of the curved quadrupole to collect the ions, and a picoammeter (Keithley 6485) is connected to the Faraday cup, which displays the current.

In addition, laser-induced fluorescence spectroscopy is employed to detect the ions and to evaluate the kinetic energy after deceleration. A laser beam with a narrow linewidth travels in the opposite direction to the decelerated ions at the exit of the quadrupole, and the $2^3P_0(F = 3/2) \rightarrow 2^3S_1(F = 5/2)$ transition of $^7Li^+$ is probed as the wavelength of the laser is scanned around 548.5 nm. The fluorescence is detected using a photomultiplier tube-based imaging system. From the Doppler shift of the line center, the axial velocity of the decelerated ions can be deduced from the formula $v = c\Delta f/f$, where f is the absolute transition frequency, Δf is the Doppler shift, and c is the speed of light in vacuum.

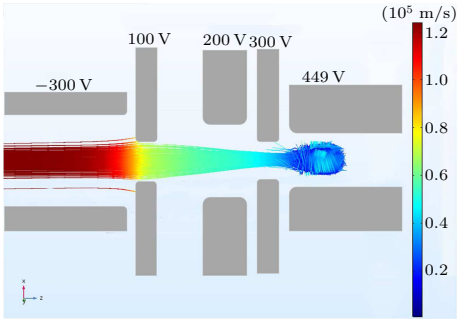

Fig. 2. Trajectories of ions in the deceleration electrodes. Movement of the ions is from left to right. Trajectories in the figure are cut off at a certain moment.

As mentioned above, there are many adjustable parameters for the deceleration device, such as the voltages applied on each electrode, and the RF. To acquire suitable parameters to start the adjustment, the electric field and ion trajectories of the deceleration system should be simulated before actual operation. Then, a physical model is built for our system. The initial kinetic energy of the Li^+ ions on entering the drift tube is set to the Gaussian distribution with an average value of 450 eV, which is in accordance with real experimental conditions. As shown in Fig. 2, with suitable voltages applied on the electrostatic lens, the ions are decelerated and focused into the quadrupole.

In addition, we considered the electric field distribution of the curved quadrupole since the curved pole leads to a product of the multipole fields,[33] and thus, the potential field deviates from the geometric center (see Fig. 3(a)).[32] The relative deviation was obtained from the simulation results by changing the curvature radius of the quadrupole (Fig. 3(b)). Notably, the deviation of the potential field increases as the curvature radius of the quadrupole decreases. Finally, the curvature radius of quadrupole R was designed to be 55 mm,

and $R/r_0 = 12.5$ (r_0 is the minimum distance between the trap axis and electrodes, as shown in Fig. 1). Thus, the relative deviation of the bottom of the potential well can be expressed as $\Delta x/r_0 \approx 0.01$, which is negligible and has almost no effect on the trajectory of the ion beam.

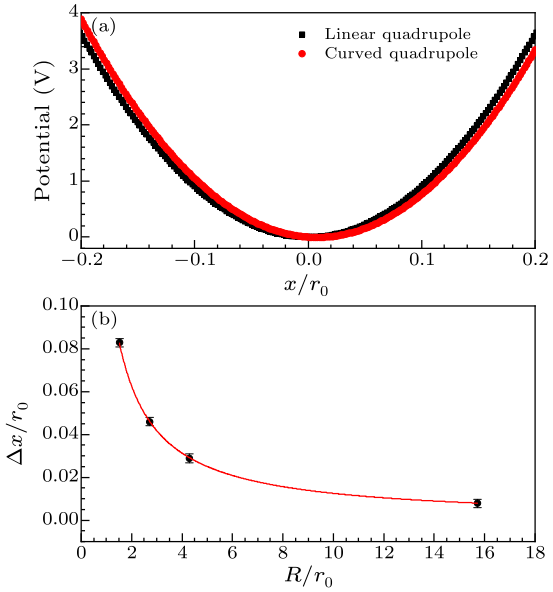

Fig. 3. Relative deviation of the potential field in the center of curved quadrupole. (a) Relative deviation of the potential when the curvature radius R is 55 mm. (b) Relative deviation of the potential field changed by R/r_0.

We then set the RF frequency $\Omega/2\pi$ to 3.46 MHz, and initial RF voltage (peak–peak amplitude) to 42 V. Under these conditions, we performed the ion trajectory simulation, which demonstrates that the ions can be decelerated and guided by the electrostatic lens and curved quadrupole trap. When the Gaussian distributed ion beam enters the deceleration lens, with proper application of voltages on the lens, part of the lower-energy ions are hindered by the electrical field, part of the higher-energy ions hit or escape from the quadrupole, and only moderate-energy ions are decelerated and guided by the quadrupole.

In our experiment, the DC voltages applied on different electrodes are set at the values shown in Fig. 2. Then, the RF frequency and RF amplitude, as well as the bias voltage, $U_{\rm bias}$, are altered to analyze the transmission efficiency and kinetic energy of the metastable ions.

The curved quadrupole can be considered as a two-dimensional ion trap, and the change from the RF frequency/amplitude of the curved quadrupole indicates the change in the stability parameters, of the trap, q, which is approximated to $2QU_{\rm rf}/Mr_0^2\Omega^2$, where Q and M are the charge and mass of the ion, respectively. We detected the ion beam behind the quadrupole trap by scanning the RF amplitude. The result indicates that the ion beam can be successfully guided through the quadrupole when q is in the range $[0.2, 0.9]$, which is in agreement with the stable region of an ideal Paul trap.[34] Thus, the curved quadrupole trap used in the experiment can be approximated by an ideal Paul trap.

By applying an RF field with a peak-to-peak voltage of 84 V and frequency ($\Omega/2\pi$) of 3.46 MHz, an ion current of approximately 30 nA was detected by the Faraday cup. Under this condition, the fluorescence profile of the transition $2^3P_0, F = 3/2 \rightarrow 2^3S_1, F = 5/2$ is shown in Fig. 4. Notably, there are multi-peaks that are not caused by hyperfine or fine splittings. This indicates that the axial kinetic energy of the decelerated ion beam has a multi-component distribution. As deduced from the Doppler shifts, the axial kinetic energy of the ion beam includes various peak components including 2.4 eV, 3.4 eV, 4.3 eV, and 6.1 eV, the minimum axial kinetic energy of the decelerated ions is ~2.4 eV, and the full width at half maximum is approximately 0.6 eV. Therefore, the decelerated ions are feasible for loading into an ion trap for further sympathetic cooling.

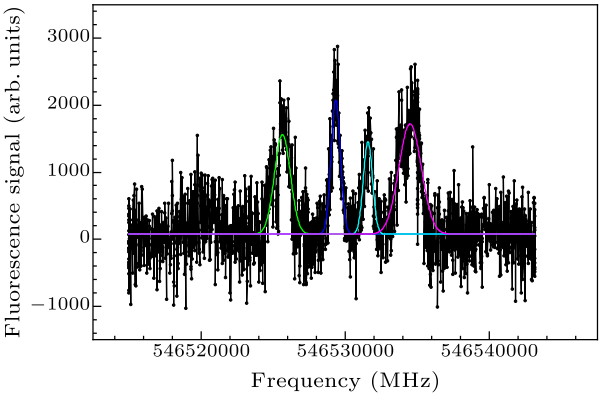

Fig. 4. Fluorescence signal of the decelerated ion beam with an RF voltage of 84 V, RF frequency of 3.46 MHz. All the peaks shown in the figure are the fluorescence signal of the transition: $2^3P_0, F = 3/2 \rightarrow 2^3S_1, F = 5/2$. The last peak corresponds to the ion energy of approximately 2.4 eV.

The complex distribution of the kinetic energy of the decelerated ions may be caused by the coupling of axial and radial motion of the ions. When ions go through the asymmetric multipole field zones, such as the curved and exit portion of the quadrupole, the radial motion of the ions is coupled with the axial motion,[35,36] while a new balance is not generally reached during the short flight time. To confirm this analysis, we performed a simulation designed for the experimental conditions and observed an inconspicuous velocity distribution of ions. Then, we changed the RF voltage applied to the quadrupole and observed that the velocity distribution of ions also changed. Figure 5 shows a simulation of the axial velocity distribution of ions when the RF voltage is set to 37 V, and the distribution is in good agreement with the experimental results when the RF voltage is 84 V.

The discrepancy may be attributed to the machining and assembling accuracy of the curved quadrupole, which may result in the unexpected multipole field. Additionally, the simulation demonstrates that when ions pass through the bent portion of the quadrupole, the axial velocity begins to show multiple components. The phenomenon is more evident at the exit of the quadrupole.

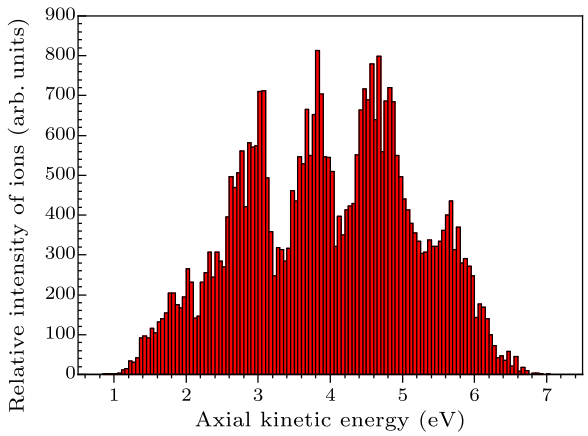

Fig. 5. Axial kinetic energy distribution of decelerated ions with an RF voltage of 37 V, and RF frequency of 3.46 MHz.

In summary, a method for decelerating ions is designed and constructed, which comprises a drift tube, an electrostatic lens, and a curved quadrupole. For demonstration of the method, a metastable Li^+ ion with kinetic energy of approximately 450 eV is decelerated to a few eV. The method can be used for loading ions into ion traps, and may be used in an ion–surface chemical reaction, state selective charge transfer, highly charged ion clock, etc. It is particularly useful in filtering out high-energy ions and neutral particles. The multi-peak velocity distribution after ion deceleration that occurred in our experiments suggests motion coupling of ions under asymmetric fields. Consequently, the coupling process is worthy of further study. The multi-components of velocity may provide a new way of researching ion–surface chemical reactions.

We thank Tingyun Shi, Zongxiu Nie, Xiaoyu Zhou and Jie Yang for the help and discussions, and Gengwu Li for careful reading of this manuscript.

References

[1] Rajput J, Roy A, Kanjilal D, Ahuja R and Safvan C 2010 *Rev. Sci. Instrum.* **81** 043301
[2] Safvan C, Rajput J, Roy A, Kanjilal D and Ahuja R 2012 *J. Phys.: Conf. Ser.* **388** 142006
[3] Lebius H, Brenac A, Huber B, Maunoury L, Gustavo F and Cormier D 2003 *Rev. Sci. Instrum.* **74** 2276
[4] Stöhlker T, Mokler P, Bosch F *et al.* 2000 *Phys. Rev. Lett.* **85** 3109
[5] Lubinski G, Juhász Z, Morgenstern R and Hoekstra R 2001 *Phys. Rev. Lett.* **86** 616
[6] Schmöger L, Schwarz M, Baumann T M, Versolato O, Piest B, Pfeifer T, Ullrich J, Schmidt P O and Crespo López-Urrutia J 2015 *Rev. Sci. Instrum.* **86** 103111
[7] Micke P, Leopold T, King S, Benkler E, Spieß L, Schmoeger L, Schwarz M, López-Urrutia J C and Schmidt P 2020 *Nature* **578** 60
[8] Kozlov M, Safronova M, López-Urrutia J C and Schmidt P 2018 *Rev. Mod. Phys.* **90** 045005
[9] Clarke J J and van Wijngaarden W A 2003 *Phys. Rev. A* **67** 012506
[10] Holt R, Rosner S, Gaily T and Adam A 1980 *Phys. Rev. A* **22** 1563
[11] Fan B, Lurio A and Grischkowsky D 1978 *Phys. Rev. Lett.* **41** 1460
[12] Kötz U, Kowalski J, Neumann R, Noehte S, Suhr H, Winkler K and zu Putlitz G 1981 *Z. Phys. A* **300** 25
[13] Chen T, Du L J, Song H F, Liu P L, Huang Y, Tong X, Guan H and Gao K L 2015 *Chin. Phys. Lett.* **32** 083701
[14] Knight R and Prior M 1980 *Phys. Rev. A* **21** 179
[15] Hijazi H and Meyer F W 2013 *Rev. Sci. Instrum.* **84** 033305
[16] Chen S, Liang S, Sun W, Huang Y, Guan H and Gao K 2019 *Rev. Sci. Instrum.* **90** 043112
[17] Budker G I 1967 *Sov. J. At. Energy* **22** 438
[18] Hänsch T W and Schawlow A L 1975 *Opt. Commun.* **13** 68
[19] Sairam T, Bhatt P, Kumar A, Kumar H and Safvan C 2015 *Phys. Plasmas* **22** 113503
[20] Zhao Q, Zhai G and Kwok R 2006 *Mater. Lett.* **60** 3084
[21] Gordon M and Giapis K 2005 *Rev. Sci. Instrum.* **76** 083302
[22] Shimizu S, Sasaki N, Ogata S and Tsukakoshi O 1996 *Rev. Sci. Instrum.* **67** 3664
[23] Foo K, Lawson R, Feng X and Lau W 1991 *J. Vac. Sci. Technol. A: Vac. Surf. Films* **9** 312
[24] Hoffman E D and Stroobant V 2007 *Mass Spectrometry: Principles Applications* (Chichester: John Wiley & Sons) vol 1
[25] Douglas D 1989 *Can. J. Spectrosc.* **34** 38
[26] Church D 1969 *J. Appl. Phys.* **40** 3127
[27] Su X, Lu W and Rabinowitz J D 2017 *Anal. Chem.* **89** 5940
[28] Bi Q R, Hou J J, Yang M, Shen Y, Qi P, Feng R H, Dai Z, Yan B P, Wang J W, Shi X J, Wu And Guo D A W Y 2017 *J. Am. Soc. Mass Spectrom.* **28** 443
[29] Rosen E P, Bokhart M T, Nazari M and Muddiman D C 2015 *Anal. Chem.* **87** 10483
[30] Aramendía M A, Marinas A, Marinas J M, Sánchez E, Urbano F J, Guillou C, Moreno Rojas J M, Moalem M and Rallo L 2010 *Rapid Commun. Mass Spectrom.* **24** 1457
[31] Yang H, Yang C and Sun T 2018 *Rapid Commun. Mass Spectrom.* **32** 1353
[32] Zhou X, Xiong C, Xu G, Liu H, Tang Y, Zhu Z, Chen R, Qiao H, Tseng Y H, Peng W P, Nie Z and Chen Y 2011 *J. Am. Soc. Mass Spectrom.* **22** 386
[33] Gravesen J and Willatzen M 2006 *Physica B* **371** 112
[34] Paul W 1990 *Rev. Mod. Phys.* **62** 531
[35] Wang Y, Huang Z, Jiang Y, Xiong X, Deng Y, Fang X and Xu W 2013 *J. Mass Spectrom.* **48** 937
[36] Hager J W 2002 *Rapid Commun. Mass Spectrom.* **16** 512